JUPITER'S IO-C AND IO-B DECAMETRIC EMISSION SOURCE MORPHOLOGY FROM LWA1 DATA ANALYSIS

K. Imai*, C. A. Higgins†, M. Imai‡, and T. E. Clarke§

Abstract

The information about Jupiter's decametric radio source locations is a very important key to understand the emission mechanism. By using the modulation lanes in the dynamic spectra of Jupiter's decametric emissions we developed a remote sensing tool to investigate Jupiter's radio source locations. This modulation lane method provides a very unique opportunity to know the source locations. Recently we have used it with data taken by the Long Wavelength Array Station 1 (LWA1). The high sensitivity of the LWA1 allows us to measure the slope of the modulation lanes more precisely for many Io–related sources in comparison to previous observations. The source locations and beam parameters can be calculated by these slope measurements. In this analysis we found the existence of two independent radio sources in the case of Io-C and Io-B events. We named the new components Io-C' (Io-C–prime) and Io-B' (Io-B–prime).

1 Introduction

Although there is a long history of Jupiter radio observations since the discovery in 1955 [Burke and Franklin, 1955], the emission mechanism of Jupiter's decametric radiation is not yet completely understood. The observed emission probability is correlated with the central meridian longitude (CML) of System III. Three main CML regions where the probability of detection is greatest have been identified and designated as sources A, B, and C [Carr et al., 1961]. It is known that the emission is elliptically or circularly polarized, in the right-hand sense for sources A and B, and often in the left-hand sense for source C. This decameter radio emission (DAM) is believed to be radiated in the R-X mode (right hand polarized extraordinary wave) at a frequency just above the local

* *Department of Elect. Engineering and Information Science, Kochi National College of Technology, Kochi, Japan*
† *Department of Physics and Astronomy, Middle Tennessee State University, Murfreesboro, TN, USA*
‡ *Department of Physics and Astronomy, University of Iowa, Iowa City, IA, USA*
§ *Remote Sensing Division, US Naval Research Laboratory, Washington, DC, USA*

electron gyrofrequency (see, for example, Carr and Desch [1976], Carr et al. [1983], Zarka [1998], and references therein). Therefore, the sources A and B are considered to be located in the northern auroral zone and the source C in the southern auroral zone. The three principal source regions A, B, and C have both Io–controlled and Io–independent components. The Jovian radio sources Io-A, Io-B, Io-C, non-Io-A, non-Io-B, and non-Io-C are defined by their locations on the CML versus Io phase (the angle of Io with respect to superior geocentric conjunction) plane [Carr and Desch, 1976]. Later the Io-D source was also identified to be left-hand circularly polarized from the summary of Carr et al. [1983].

The modulation lanes in the dynamic spectra of Jupiter's decametric radio emissions were discovered by Riihimaa [1968]. At frequencies in the vicinity of 22 MHz, most modulation lane patterns have frequency–time slopes between +100 and +180 kHz/sec for Io-B storms and between −90 and −150 kHz/sec for Io-A storms. The lanes generally display a strong periodicity in time, with periods ranging from about 1 to 5 s and an average of about 2 s. We developed a model for the mechanism responsible for their production to provide a very close fit with the observations for the first time [Imai et al., 1992a; 1992b; 1997]. In this model, the slope of the modulation lanes provides important information to know the radio source locations. By using the measured slope of modulation lanes it is possible to make calculations of the source locations based on Jupiter's magnetic field model. This remote sensing tool is called the modulation lane method [Imai et al., 2001; 2002; 2006].

The Long Wavelength Array (LWA) is a low-frequency radio telescope designed to produce high sensitivity, high resolution spectra in the frequency range of 10–88 MHz. The Long Wavelength Array Station 1 (LWA1) is the first LWA station completed in April 2011, and it is located near the VLA site in New Mexico, USA. LWA1 consists of a 256 element array operating as a single–station telescope. The sensitivity of the LWA1, combined with the low radio frequency interference environment, allows us to observe the fine structure of Jupiter's decametric modulation lanes [Clarke et al., 2014]. Using newly available wide band modulation lane data observed by LWA1, we calculated source locations and beam parameters based on the modulation lane method.

2 Radio source parameters

It is generally agreed that Jupiter's decametric radiation is emitted into a thin conical sheet that is more or less in the form of a hollow cone. It is composed of ray vectors making angles somewhat less than 90° with respect to the magnetic field in the region. As shown in Figure 1, Io-B activity is observed when one limb of the hollow cone intersects the Earth direction, and Io-A when the other limb of the cone is toward Earth.

Two conditions for emission to occur are: *a*) the emitting region near the foot of the flux tube passing through it must have received Alfvén wave energy introduced earlier by magnetospheric corotation past Io, and *b*) this emitting region must lie within the so-called active longitude zone centered near the longitude of the Jovian north or south magnetic pole. As magnetic field lines sweep by Io in succession, the resulting Alfvén wave energy introduced into them propagates down to the emission region, so that the emission process

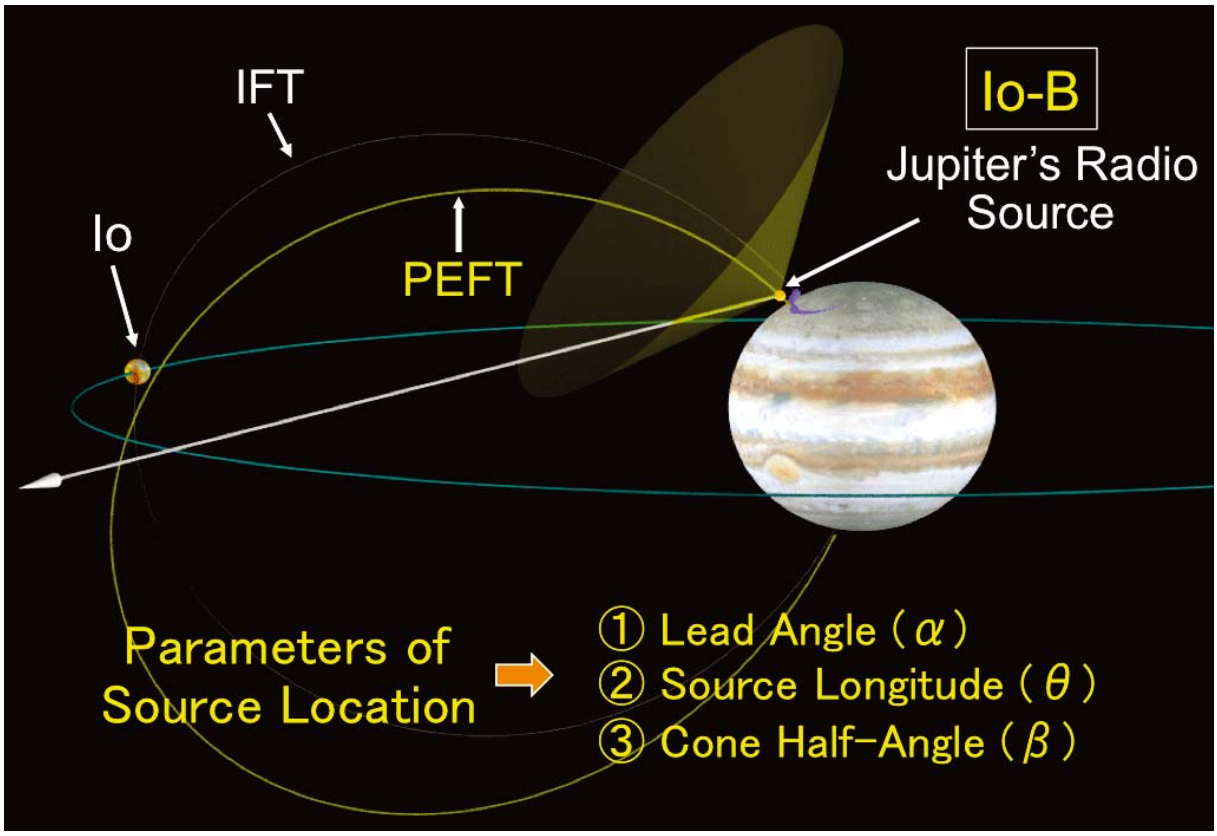

Figure 1: Source parameters of Jupiter's decametric radio emissions in the case of Io-B source geometry. IFT and PEFT are the abbreviations for Io flux tube and previously energized flux tube, respectively.

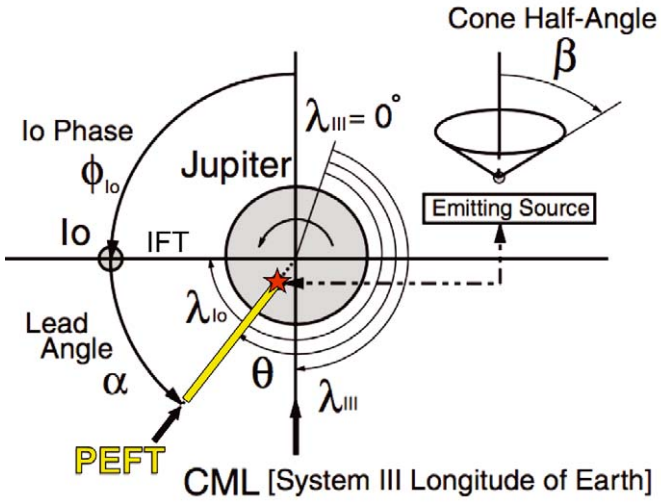

Figure 2: Geometry of Io-B source in a section through the Jovian equator. The figure shows the geometrical parameters of lead angle α, source longitude θ, and cone half-angle β.

continues until the boundary of the active longitude zone has been crossed. Thus, as long as the radio emitting region is active, its Jovian longitude leads the sub-Io longitude

(Jovian System III longitude of Io's position) by an approximate fixed amount. The value of this lead angle has not been directly measured because of the lack of knowledge of the mean velocity of the Alfvén waves in the Io flux tubes.

As shown in Figure 1, we refer to the flux tube passing through Io at a given time as the Io flux tube (IFT), and to the flux tube from the foot of which radiation is being emitted at the same time as the previously energized flux tube (PEFT). Figure 2 shows the lead angle α between IFT and PEFT. λ_{III} (synonymous with CML) is the Jovian west longitude of the central meridian of the planet as viewed from Earth. The longitude of Io is λ_{Io}. Angle θ is the longitude of the intersection of the active magnetic flux tube with the equatorial plane. The orbital phase of Io from superior geocentric conjunction is ϕ_{Io}. Once the location of the source (θ) is found, we determine the cone half-angle β as the angle between the direction tangent to the magnetic field line at the source and the direction to Earth as seen from the source.

3 Modulation lane method

The details of the modulation lane method are described by Imai et al. [1997; 2002; 2006]. In this section we briefly review this modulation lane method. In Figure 3 (left), we show a geometry of our modulation lane model for the Io-B source. We consider a grid–like interference screen composed of field-aligned columns of enhanced or depleted plasma density located along the longitudinal direction near satellite Io's orbit which is close to the high density part of Io Plasma Torus (Region of the Io Plasma Ribbon [Schneider and Trauger, 1995]).

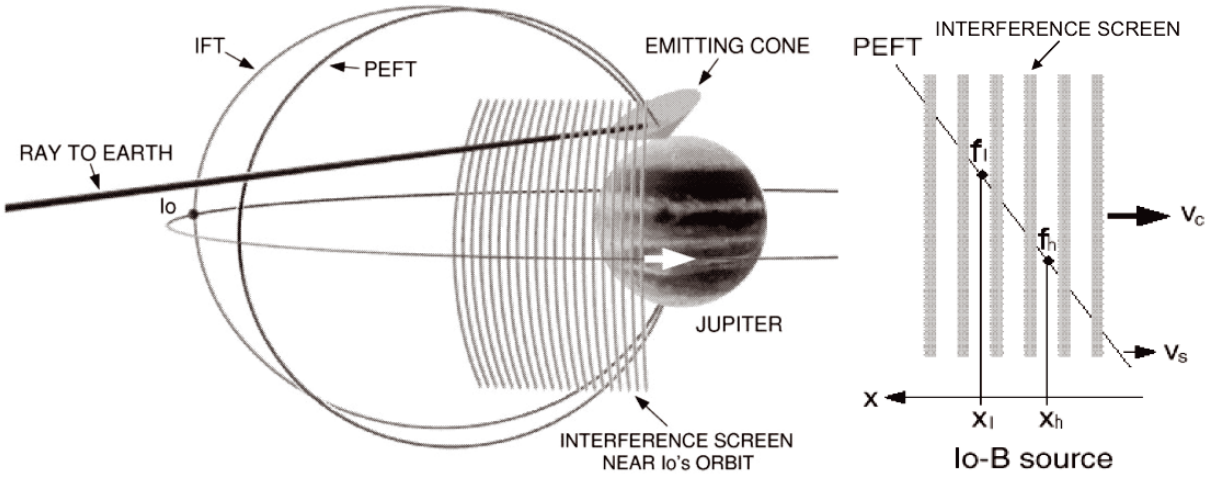

Figure 3: Left: Geometry of our modulation lane model for the case of the Io-B source. The indicated column spacings in the interference screen are an idealized model; they don't represent a real scale size. Right: Diagram illustrating the origin of the slope of a modulation lane for Io-B. This plot is a projection on a plane perpendicular to the ray to Earth.

Figure 3 (right) shows two points on the active flux tube (PEFT) from which radiation is being emitted at the frequencies f_h and f_l, where f_h is the higher frequency. We define

the positive x direction to be perpendicular to the line of sight to Earth and parallel to the Jovian equator, in the direction of increasing System III (west) longitude. Let the x coordinates of the above two points be x_h and x_l, respectively. The angular velocity of the plasma column system with respect to the radio source is $(v_c - v_s)/r$, where v_s and v_c are the x-components of the velocities of the radio source and the plasma columns located between it and Earth, and r is the distance from the source to the columns. The frequency–time slope of a modulation lane over the frequency interval between f_l at t_l and f_h at t_h is defined to be $SL = (f_h - f_l)/(t_h - t_l)$. Since $t_h > t_l$ for Io-B modulation lanes and $t_h < t_l$ for Io-A, SL is positive for the former and negative for the latter. The frequency–time slope equation can be written in the form

$$SL = -\frac{(v_c - v_s)\ (f_h - f_l)}{(x_h - x_l)}\ . \tag{1}$$

This equation is used in the generation of modeled modulation lanes for comparison with observed data. The detail of this computer simulation is explained in Imai et al. [2002].

Figure 4 shows the wide band Io-B modulation lanes observed by LWA1. The frequency–time slope is positive, and the lane curvature is apparent. Major modulation lanes can be seen cutting across the minor lanes which have opposite slope and more irregular structure.

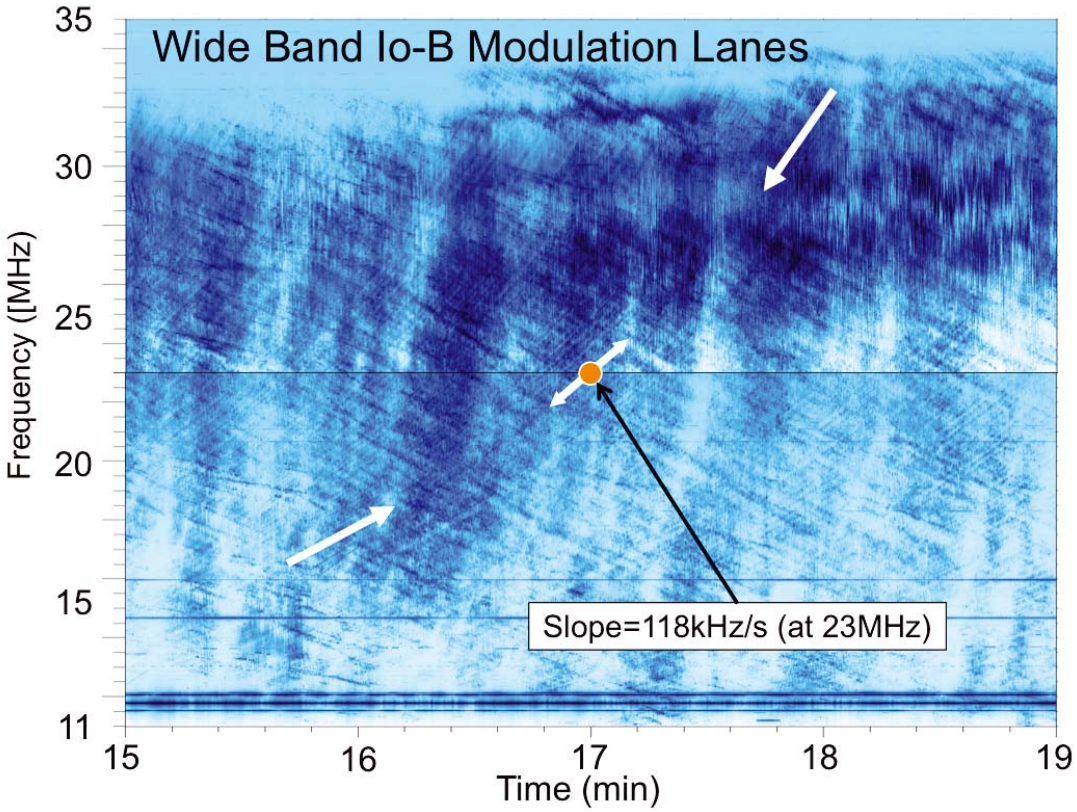

Figure 4: Wide band modulation lanes of the Io-B source from 12 MHz to 34 MHz observed by LWA1 on 30 December, 2013 from 10:15 to 10:19 UT. The blue scale shows Stokes I power spectral density in arbitrary units.

This event was very unique showing curved modulation lanes over a 22 MHz frequency bandwidth from 12 MHz to 34 MHz. By using our modulation lane method based on Equation (1) we can calculate these curved modulation lanes to fit the observed ones with specific lead angle α. This is called the curvature fitting method which is the most accurate way to determine the value of the lead angle α (see Figure 4, Imai et al. [2002]). However these wide band modulation lanes are not commonly observed. Thus we usually measure the slope with a 1 MHz bandwidth and then we determine the most probable value of the lead angle α to fit the value of the slope based on Equation (1).

Table 1: Measured slope and derived source parameters using different magnetic field models.

	VIP4			VIPAL			O6		
Slope	α	θ	β	α	θ	β	α	θ	β
130 kHz/s	56°	170°	58°	54°	172°	56°	58°	168°	55°
118 kHz/s	49°	177°	61°	47°	179°	59°	52°	174°	58°
106 kHz/s	39°	187°	67°	36°	190°	65°	43°	183°	62°

In the case of Figure 4 we measured the value of the slope of the modulation lanes as 118 kHz/s centered at 23 MHz with 1 MHz bandwidth. We used these data to check the accuracy and the dependence on the Jovian magnetic field model. Table 1 shows the measured slope and the derived source parameters using different magnetic field models, like VIP4, VIPAL, and O6. We can usually measure the slope within 10% accuracy; therefore, we also added the values of 130 kHz/s (+10%) and 106 kHz/s (−10%) into Table 1.

By using the VIP4 Jovian magnetic field model we derived the source parameters as the lead angle α=49°, the source longitude θ=177°, and cone half-angle β=61°. From Table 1 we understand these derived values have no significant difference with different magnetic field models and the deviations of the derived values with ±10% slope reading accuracy can be estimated. As long as we use the same Jovian magnetic field model to derive the source parameters, we can conduct the systematic investigation of the radio source locations.

In case of the modulation lane method, the lead angle is a free parameter to fit the slope of the modulation lanes. Our results [Imai et al., 1997] show the lead angle is usually variable and the cone half-angle is almost fixed for the case of Io-B and Io-A sources. The range of the lead angle value of Io-B and Io-A sources are from 30° to 70° and 0° to 50°, respectively [see Table 1, Imai et al., 1997]. Leblanc et al. [1994] concluded that the lead angle is 16° to 42° for the Io-B source based on the polarization measurements which were made by a very different method. The derived lead angle by Hess at al. [2010] was about 0 to 10° for Io-C and Io-D arcs. It was based on the comparison between the observed arc structures of the Jovian dynamic spectra and the modeled arc calculated by a loss cone driven electron cyclotron maser instability theory. In this approach they used the theoretical beaming angle profile to fit the arc structure. In our case we consider a simple geometrical radio ray direction. So far the lead angle values obtained by several authors are not in good agreement.

4 Io-C source morphology

Figure 5 shows a typical dynamic spectrum of the Io-C source emission observed by LWA1. In case of Io-C we sometimes see mixed polarization components with left-hand polarization (LH: blue) and right-hand polarization (RH: red). In Figure 5 it is very clear that the CML range of Io-C LH component is from 230° to 340° at 13 MHz. The peak frequency is about 24 MHz at approximately 290° CML.

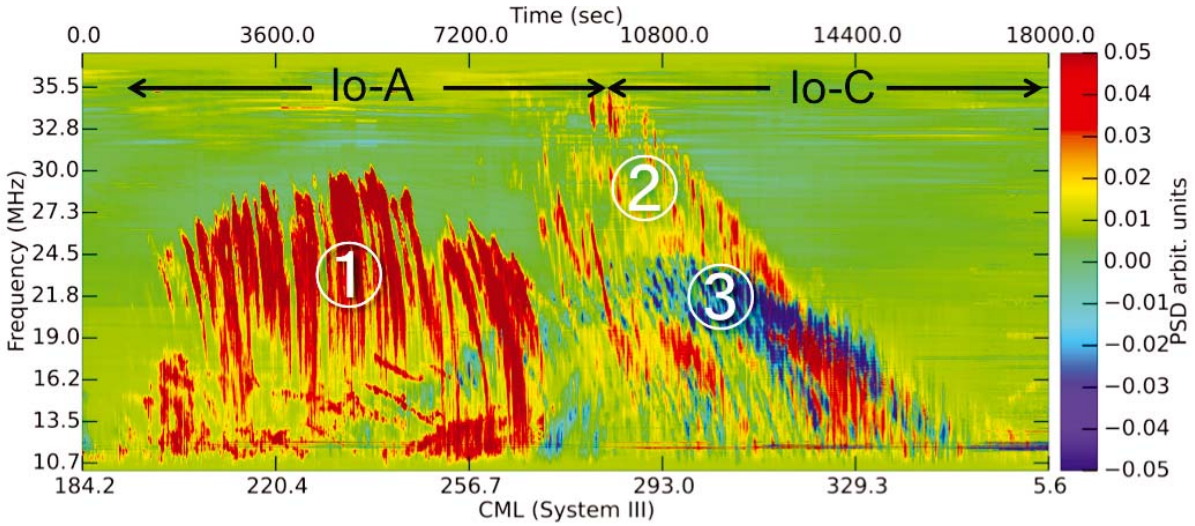

Figure 5: Jupiter Io-A/Io-C emission on 1 December, 2012 beginning at 08:14 UT. Io-A (Part 1) and Io-C (Part 2) are right-hand circularly polarized (red) and Io-C (Part 3) is left-hand circularly polarized (blue). The 5-hour observation shows a frequency range from 10 to 37 MHz, a CML range of 184.2°-5.6°, and a corresponding ϕ_{Io} from 211°-254°. The colorbar shows Stokes V power spectral density in arbitrary units.

The peak frequency of the Io-C RH component in Figure 5 is about 35 MHz at around 280° CML value. This peak frequency is much higher than Io-C LH case. The same observational results have been reported by Boudjada et al. [1996] by using the Nançay Decametric Array. The interesting part of Io-C is the cross-section of the LH and RH components during the CML range from about 300° to 330°. If we can use our modulation method for the overlapping regions of the LH and RH components, the derived source locations of these components can be compared to further investigate the Io-C source morphology. Figure 6 shows four different examples of dynamic spectra of the Io-C source with both LH and RH components. These CML ranges are from 298° to 326°, and the Io Phase ranges are from 236° to 241°.

In Figure 6 we identified the modulation lanes for both LH (red) and RH (green) components in each plot. It is clear the different modulation lane patterns exist between the LH and RH components. Since they have no correlations with each other, each polarization component must be radiated independently. By using our modulation lane method we measured the slope within a 1 MHz bandwidth at an appropriate observing frequency. In this calculation to derive the source parameters based on the R-X mode radiation, we take into account the northern hemisphere side PEFT for RH modulation lanes and the southern hemisphere side PEFT for LH modulation lanes.

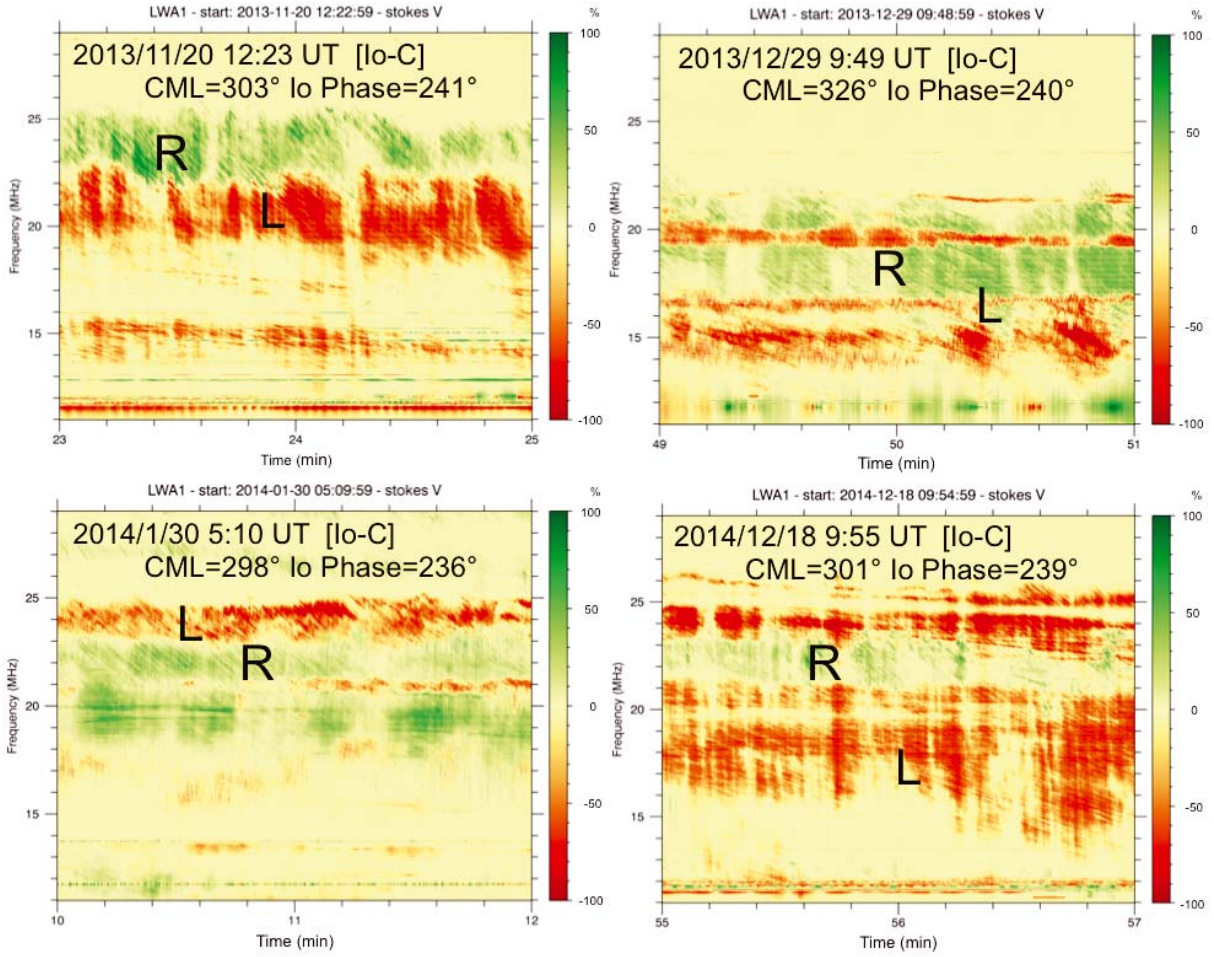

Figure 6: Four plots of independent Io-C events which have overlapping regions of LH (red) and RH (green) components. Each plot shows the dynamic spectrum including the LH and RH modulation lanes during 2 minutes. The colorbar shows Stokes V power spectral density in arbitrary units.

The statistical results of these four cases of LH component show that the mean value of the source longitude θ is 248° (the standard deviation, $\sigma = 10.4°$), and the cone half-angle β is 71° ($\sigma = 1.3°$). And the results for RH component show that the mean θ is 285° ($\sigma = 8.3°$), and the cone half-angle β is 60° ($\sigma = 2.6°$). These results indicate that the source longitudes of the LH and RH components of the Io-C source are different, and the values of the cone half-angle are also different. It means that two independent radio sources exist in the Io-C source regions. So we specifically name the Io-C' (Io-C–prime) for the RH component of the Io-C source. The physical process of the association with both the LH and RH components is not well known. But the mean source longitude of Io-C', 285°, is close to the value of 290° which is the brightness peak of the IFP (Io footprint) when Io is close to the Io plasma torus center [Bonfond et al., 2013]. This information may be very important to study the physical process for future work.

5 Io-B source morphology

Figure 7 shows four different examples of dynamic spectra of the Io-B source observed by LWA1. The CML ranges of the four plots are almost the same from about 60° to 210°. To investigate the Io-B source morphology we measured the slope of the modulation lanes for these four cases with a 1 MHz bandwidth at an appropriate observing frequency. In Figure 7 we show the frequency/time points where the slopes were measured by orange dots in each plot.

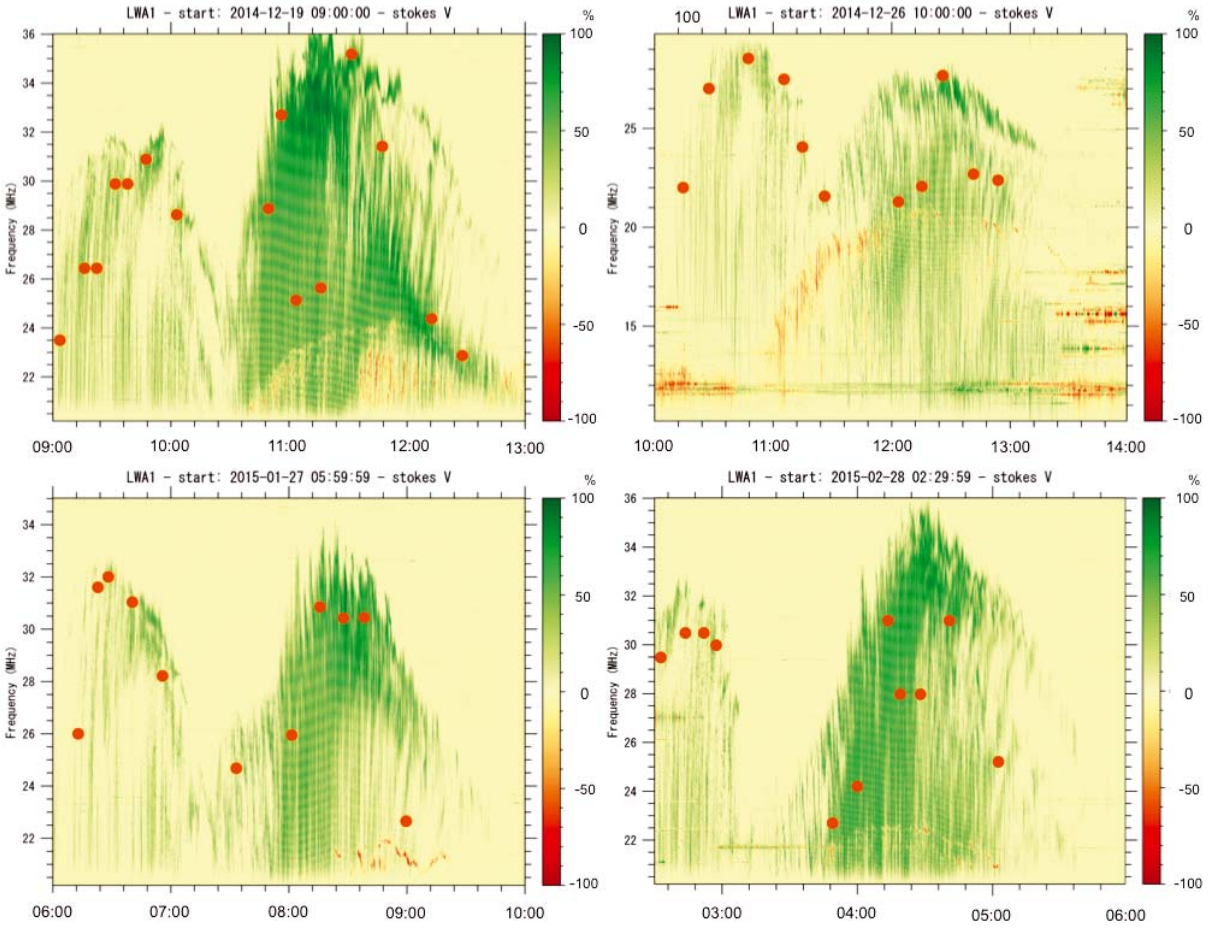

Figure 7: Four independent dynamic spectra of Io-B events (RH: green) that have 4-hour durations. The colorbar shows Stokes V power spectral density in arbitrary units. The positions of measured slopes of modulation lanes are marked by orange dots. The modulation lanes are not visible in this spectrum due to the low time resolution. The LH (Red) emission is also identified from the Io-D source. The horizontal interference patterns in the Io-B emission are due to the Faraday effect.

From Figure 7 we identified two distinct parts (each part has the independent peak of the emission frequency) that exist in the Io-B source. One is the main part of Io-B between about 110° to 180° CML. The other is the early part of Io-B between about 60° to 110° CML. This early part is a very weak region in comparison with the main part. We can see the details of this early part by virtue of the high sensitivity of the LWA1. During

the 2014–2015 observing season of LWA1 we identified these four cases from seven Io-B events. The observed Io Phase range of the four cases is limited from about 65° to 85°.

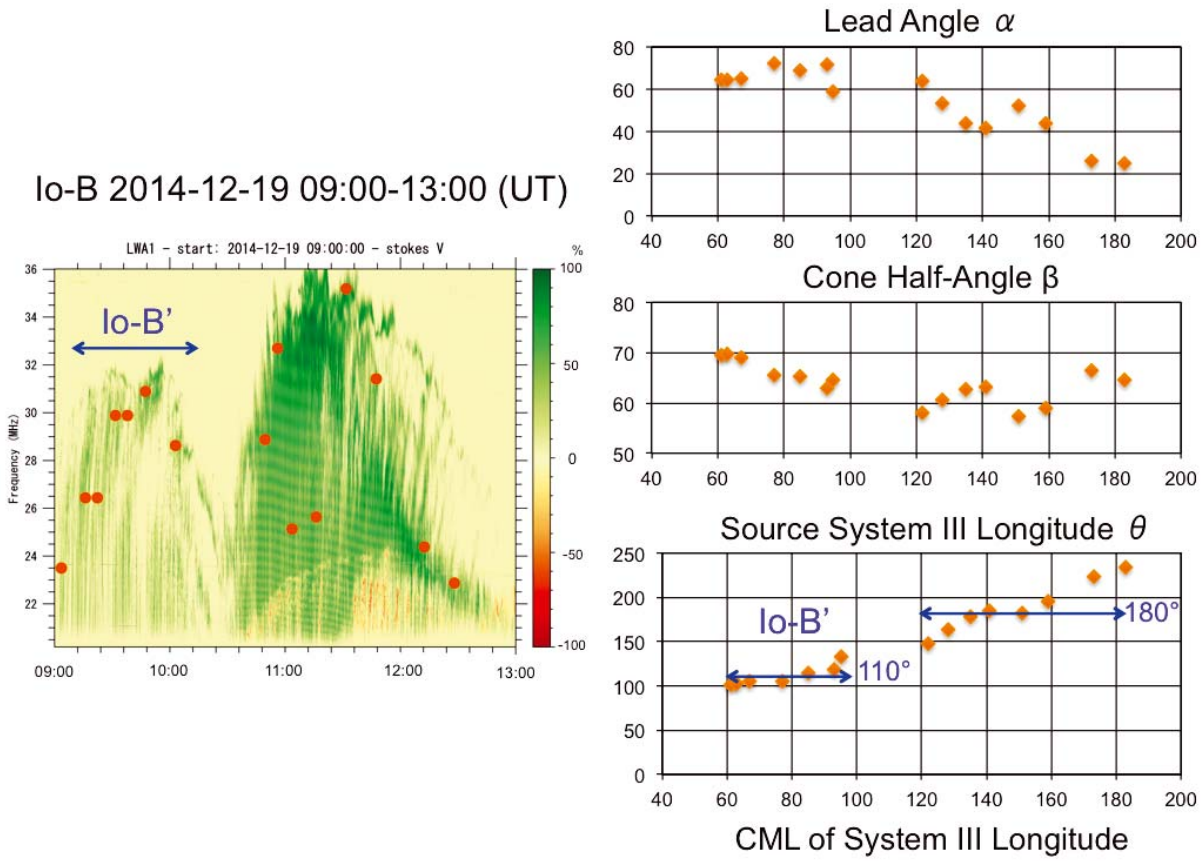

Figure 8: Left: Io-B event (indicating the range of Io-B') on 19 December, 2014 from 09:00 to 13:00 UT (CML=58°-204°, ϕ_{Io}=75°-109°) observed using LWA1 spectrometer mode at 40 ms and 20 kHz resolution. The frequency range is from 20 to 36 MHz. Right: Derived source parameters, Lead angle α, Cone half-angle β, Source System III longitude θ. The center of the source longitude ranges are also indicated as 110° *and* 180°.

Figure 8 shows one of four events in Figure 7 and the derived source parameters, lead angle α, cone half-angle β, and source System III longitude θ plotted in association with the CML of System III longitude by using the modulation lane method. From the plot of the source System III longitude the measured center of the source longitude range is about 110° in the case of the early part of Io-B and about 180° in the case of the main part. The other three Io-B events in Figure 7 show the same trend for the center of the source longitude. It means two independent radio active regions exist in the Io-B source. So we name the Io-B' (Io-B–prime) for this early part of the Io-B region. This 110° source longitude corresponds to the brightness peak of the IFP (Io footprint) when Io is close to the Io plasma torus center [Bonfond et al., 2013]. Also the 180° source longitude of the main part in Io-B source is close to the center of the longitude range of the active magnetic flux tube for non-Io–related radio emissions [M. Imai et al., 2011].

The important point is that four independent events show very similar characteristics such as the two parts of spectral pattern and the different source System III longitude range

calculated by the slope of the modulation lanes (each individual slope is different because of a different measuring frequency). In addition, this Io-B' region seems to be restricted within 60° to 110° and Io phase 65° to 85°. These characteristics are not present in other Io–controlled decameter storms like Io-A and Io-C.

Recently Marques et al. [2017] show new emission types (Io-A" and Io-B') based on the statistical analysis of 26 years of observations with the Nançay Decameter Array. They argue that Io-A" has the same RH polarization as Io-A and also starts at a CML region that is still well in the Io-A source region. Our Io-C' classification is based on the modulation lane data analysis and corresponds to their Io-A". The difference in classification is based on the range of the CML longitude and whether it falls within the known longitude of the C source region. On the other hand our Io-B' seems to be different from their Io-B'. Their Io-B' has a higher CML range (100° to 200°), but in our case, the Io-B' corresponds to the early part of the CML range (60° to 110°). The reason is that our data analysis of the modulation lanes includes the very weak part of the Io-B source. This part can only be seen by high sensitivity radio telescopes like the LWA1. With more sensitive telescopes and long term data archives, it is apparent that a consistent nomenclature of radio sources should be established.

6 Conclusions

The results of LWA1 data analyses indicate that the radio emitting sources are located along a restricted range of Jupiter's System III longitude. We only receive one of the individual sources at a given time because the source has a very thin beam (probably less than few degrees). We show the calculated locations of Io–related sources based on the modulation lanes observed by LWA1. In this analysis we identified the existence of two independent radio sources in the case of Io-C events, one from the northern hemisphere (right hand polarization; we named it Io-C', Io-C–prime), and one from the southern hemisphere (left hand polarization, Io-C). We also identified the radio source of the early part of Io-B (we named it Io-B', Io-B–prime). The Io-B' is located between about 60° to 110° CML of System III longitude and is independent of the main part of Io-B. The measured center of the source longitude range is about 110° for the case of Io-B' and 285° for Io-C'. These values are very close to the source longitudes of the brightness peak of the IFP. This information may be very important to consider the enhancement of Io-B' and Io-C' radio emissions.

Acknowledgments: We would like to thank Yusei Nakayama for his contribution to this project. This work was supported by JSPS KAKENHI Grant Number JP16K05570. We also wish to thank the staff of the Long Wavelength Array. Basic research in Radio Astronomy at the US Naval Research Laboratory is supported by 6.1 Base Funding. Construction of the Long Wavelength Array Station 1 (LWA1) was supported by the Office of Naval Research under contract N00014-07-C-0147. Support for operations and continuing development of LWA1 is provided by the National Science Foundation under grants AST-1139963 and AST-1139974 of the University Radio Observatories program. The Editors thank two anonymous reviewers for their help in evaluating this paper.

References

Bonfond, B., S. Hess, J.–C. Gérard, D. Grodent, A. Radioti, V. Chantry, J. Saur, S. Jacobsen, and J. T. Clarke, Evolution of the Io footprint brightness I: Far–UV observations, *Planet. Space Sci.*, **88**, 64–75, 2013.

Burke, B. F., and K. L. Franklin, Observations of a variable radio source associated with planet Jupiter, *J. Geophys. Res.*, **60**, 213–217, 1955.

Boudjada, M. Y., P. Galopeau, and H. O. Rucker, Jovian S-bursts: A discussion on the S-burst drift model, *Astron. Astrophys.*, **306**, L9–L12, 1996.

Carr, T. D., A. G. Smith, H. Bollhagen, N. F. Six, and N. E. Chatterton, Recent decameter–wavelength observations of Jupiter, Saturn and Venus, *Astrophys. J.*, **134**, 105–125, 1961.

Carr, T. D., and M. D. Desch, Recent decametric and hectometric observations of Jupiter, in *Jupiter*, edited by T. Gehrels, University of Arizona Press, Tucson, USA, 693–735, 1976.

Carr, T. D., M. D. Desch, and J. K. Alexander, Phenomenology of magnetospheric radio emissions, in *Physics of the Jovian Magnetosphere*, edited by A. J. Dessler, Cambridge University Press, New York, USA, 226–284, 1983.

Clarke, T. E., C. A. Higgins, J. Skarda, K. Imai, M. Imai, F. Reyes, J. Thieman, T. Jaeger, H. Schmitt, N. P. Dalal, J. Dowell, S. W. Ellingson, B. Hicks, F. Schinzel, and G. B. Taylor, Probing Jovian decametric emission with the Long Wavelength Array station 1, *J. Geophys. Res.*, **119**, 9508–9526, 2014.

Hess, S. L. G., A. Pétin, P. Zarka, B. Bonford, and B. Cecconi, Lead angles and emitting electron energies of Io–controlled decameter radio arcs, *Planet. Space Sci.*, **58**, 1188–1198, 2010.

Imai, K., L. Wang, and T. D. Carr, A model for the production of Jupiter's decametric modulation lanes, *Geophys. Res. Lett.*, **19**, 953–956, 1992a.

Imai, K., L. Wang, and T. D. Carr, Origin of Jupiter's decametric modulation lanes, in *Planetary Radio Emissions III*, edited by H. O. Rucker, S. J. Bauer, and M. L. Kaiser, Austrian Academy of Sciences Press, Vienna, 69–90, 1992b.

Imai, K., L. Wang, and T. D. Carr, Modeling Jupiter's decametric modulation lanes, *J. Geophys. Res.*, **102**, 7127–7136, 1997.

Imai, K., F. Reyes, and T. D. Carr, Modulation lane measurements of Jupiter's Io–B source parameters, in *Planetary Radio Emissions V*, edited by H. O. Rucker, M. L. Kaiser, and Y. Leblanc, Austrian Academy of Sciences Press, Vienna, 119–126, 2001.

Imai, K., J. J. Riihimaa, F. Reyes, and T. D. Carr, Measurement of Jupiter's decametric radio source parameters by the modulation lane method, *J. Geophys. Res.*, **107**, A6, id.1081, 2002.

Imai, K., F. Reyes, T. D. Carr, and A. Lecacheux, Recent progress in the measurement of Jupiter's decametric radio source parameters by the modulation lane method, in *Planetary Radio Emissions VI*, edited by H. O. Rucker, W. S. Kurth, and G. Mann, Austrian Academy of Sciences Press, Vienna, 213–221, 2006.

Imai, M., K. Imai, C. A. Higgins, and J. R. Thieman, Comparison between Cassini and Voyager observations of Jupiter's decametric and hectometric radio emissions, *J. Geophys. Res.*, **116**, A12233, 2011.

Leblanc, Y., G. A. Dulk, and F. Bagenal, On Io's excitation and the origin of Jupiter's decametric radiation, *Astron. Astrophys.*, **290**, 660–673, 1994.

Marques, M. S., P. Zarka, E. Echer, V. B. Ryabov, M. V. Alves, L. Denis, and A. Coffre, Statistical analysis of 26 yr of observations of decametric radio emissions from Jupiter, *Astron. Astrophys.*, **604**, A17, 2017.

Riihimaa, J. J., Structured events in the dynamic spectra of Jupiter's decametric radio emission, *Astron. J.*, **73**, 265–270, 1968.

Schneider, N. M., and J. T. Trauger, The structure of the Io torus, *Astrophys. J.*, **450**, 450–462, 1995.

Zarka, P., Auroral radio emissions at the outer planets: Observations and theories, *J. Geophys. Res.*, **103**, 20159–20194, 1998.